

Linear Discontinuous Expansion Method using the Subcell Balances for Unstructured Geometry S_N Transport

*Ser Gi Hong, Jong Woon Kim, Young Ouk Lee, and Kyo Youn Kim

^aKorea Atomic Energy Research Institute, Duckjin-dong, Yuseong-gu, Daejeon, Korea

*Corresponding author: hongsg@kaeri.re.kr

1. Introduction

The subcell balance methods^{1,2,3} have been developed for one- and two-dimensional S_N transport calculations. In this paper, a linear discontinuous expansion method using sub-cell balances (LDEM-SCB) is developed for neutral particle S_N transport calculations in 3D unstructured geometrical problems. At present, this method is applied to the tetrahedral meshes. As the name means, this method assumes the linear distribution of the particle flux in each tetrahedral mesh and uses the balance equations for four sub-cells of each tetrahedral mesh to obtain the equations for the four sub-cell average fluxes which are unknowns. This method was implemented in the computer code MUST (Multi-group Unstructured geometry S_N Transport). The numerical tests show that this method gives more robust solution than DFEM⁴(Discontinuous Finite Element Method).

2. Theory and Method

The starting equation is the neutral particle transport equation given by

$$\hat{\Omega}_m \cdot \nabla \varphi_{m,g}(\vec{r}) + \sigma_g \varphi_{m,g}(\vec{r}) = q_{m,g}, \quad (1)$$

where m and g mean the directions of neutral particle and the energy group, respectively. The source term q represents the scattering source plus the external source. LDEM-SCB assumes the following linear distribution of flux in each tetrahedron :

$$\varphi_{m,g}(\vec{r}) = \psi_{m,g,1} + \psi_{m,g,2}x + \psi_{m,g,3}y + \psi_{m,g,4}z, \quad (2)$$

where x, y, z are a local coordinates system whose origin is located in the center of the tetrahedron. This local coordinates system simplifies the derivation of the method. The tetrahedron is divided into its four sub-cells sharing the center point of the original tetrahedron. Next, the sub-cell average fluxes are evaluated by using Eq.(2) and the resulting relations are given by

$$\psi_{m,g,si} = \psi_{m,g,1} - \frac{1}{4}x_i\psi_{m,g,2} - \frac{1}{4}y_i\psi_{m,g,3} - \frac{1}{4}z_i\psi_{m,g,4}, i=1,\dots,4, \quad (3)$$

where (x_i, y_i, z_i) represents the coordinates of the four nodes of the tetrahedron. The four external faces of the tetrahedron are also evaluated and they are given by

$$\psi_{m,g,ei} = \psi_{m,g,1} - \frac{1}{3}x_i\psi_{m,g,2} - \frac{1}{3}y_i\psi_{m,g,3} - \frac{1}{3}z_i\psi_{m,g,4}, i=1,\dots,4, \quad (4)$$

where $\psi_{m,g,ei}$ is the average flux over the face which doesn't contain the node i . These evaluations can be done for the remaining six internal faces. For example, the average flux over the internal face composed of the

nodes 1,2,5 (origin of the local coordinates system) is given by

$$\psi_{m,g,125} = \psi_{m,g,1} + \frac{1}{3}(x_1 + x_2)\psi_{m,g,2} + \frac{1}{3}(y_1 + y_2)\psi_{m,g,3} + \frac{1}{3}(z_1 + z_2)\psi_{m,g,4}, \quad (5)$$

In fact, these above evaluations are done by using the transformation into the barycentric coordinates for simplification. The next step is to represent the face average fluxes in terms of the sub-cell average fluxes. It can be done by using the evaluations performed above. The average fluxes over the four external faces are given by

$$\psi_{m,g,ei} = \frac{15}{12}\psi_{m,g,si} - \frac{1}{12}(\psi_{m,g,\alpha} + \psi_{m,g,\beta} + \psi_{m,g,\gamma}), \quad (6)$$

where α, β, γ are the three numbers which are different from i . The fluxes for the six internal faces are given by

$$\psi_{m,g,\alpha\beta\gamma} = \frac{11}{12}(\psi_{m,g,\gamma} + \psi_{m,g,\delta}) - \frac{5}{12}(\psi_{m,g,\alpha} + \psi_{m,g,\beta}) \quad (7)$$

The final step is to substitute Eq.(6) and Eq.(7) into the four sub-cell balance equations. For example, the balance equation for the sub-cell composed of the nodes 2,3,4 and 5 is given by

$$\begin{aligned} &\hat{n}_{234} \cdot \hat{\Omega}_m A_{234} \delta_{m,234}^o \psi_{m,g,e1} + \hat{n}_{245} \cdot \hat{\Omega}_m A_{245} \psi_{m,g,245} \\ &+ \hat{n}_{345} \cdot \hat{\Omega}_m A_{345} \psi_{m,g,345} + \hat{n}_{235} \cdot \hat{\Omega}_m A_{235} \psi_{m,g,235} + \sigma_g V_{s1} \psi_{m,g,s1} = \\ &q_{s1} V_{s1} - (1 - \delta_{m,234}^o) \hat{n}_{234} \cdot \hat{\Omega}_m A_{234} [\lambda \psi_{m,g,e1}^{up} + (1 - \lambda) \psi_{m,g,e1}] \end{aligned} \quad (8)$$

where \hat{n}_{234} and A_{234} are the outward normal vector and the area of the surface composed of the nodes 2, 3, and 4, respectively. The $\delta_{m,234}^o$ is unity if the surface composed of the nodes 2,3, and 4 is an outgoing face and it is zero if the surface is an incoming face. The parameter λ is introduced to use the weighted average of the incoming external face flux from the upstream cell and the one from the present cell. It should be noted that this term is non-zero only when the external face is an incoming face. The substitution of Eq.(6) and (7) into Eq.(8) gives

$$\begin{aligned} &\left\{ \frac{15}{12} \delta_{m,234}^o - \frac{11}{12} + \frac{15}{12} (1 - \delta_{m,234}^o) (1 - \lambda) \right\} t_{m,234} + \sigma_g V_{s1} \psi_{m,g,s1} \\ &+ \left\{ \left[-\frac{1}{12} \delta_{m,234}^o + \frac{5}{12} - \frac{1}{12} (1 - \delta_{m,234}^o) (1 - \lambda) \right] t_{m,234} + \frac{16}{12} t_{m,345} \right\} \psi_{m,g,s2} \quad (9) \\ &+ \left\{ \left[-\frac{1}{12} \delta_{m,234}^o + \frac{5}{12} - \frac{1}{12} (1 - \delta_{m,234}^o) (1 - \lambda) \right] t_{m,234} + \frac{16}{12} t_{m,245} \right\} \psi_{m,g,s3} \\ &+ \left\{ \left[-\frac{1}{12} \delta_{m,234}^o + \frac{5}{12} - \frac{1}{12} (1 - \delta_{m,234}^o) (1 - \lambda) \right] t_{m,234} + \frac{16}{12} t_{m,235} \right\} \psi_{m,g,s4} \\ &= q_{s1} V_{s1} - (1 - \delta_{m,234}^o) \lambda t_{m,234} \psi_{m,g,e1}^{up} \end{aligned}$$

where $t_{m,234} = \hat{n}_{234} \cdot \hat{\Omega}_m A_{234}$.

The computational procedure is similar to those of DFEM.

4. Numerical Test and Discussion

To test the LDEM-SCB, we developed a simple mesh generator for cubic boxes. Basically, this generates six tetrahedrons of equal volume per one cubic box. We considered a cube problem which is defined by $[0 < x < 20\text{cm}]$, $[0 < y < 5\text{cm}]$, and $[0 < z < 5\text{cm}]$. This problem is divided into four coarse cubes of equal volume. These four cubes are numbered by 1, 2, 3, and 4 such that the cube 1 is leftmost and the cube 4 is rightmost along x-axis. The homogeneous neutron sources of 10.0 and 5.0 $\text{n/cm}^3\text{sec}$ are given in the cubes 1 and 2, respectively. For this problem, the five different cases of mesh divisions are considered to assess the accuracy of LDEM-SCB. The first, second, third, fourth, and fifth cases divide the problem into 24, 192, 1536, 12288, and 98304 tetrahedrons of equal volume, respectively. They correspond to 5cm, 2.5cm, 1.25cm, 0.625cm, and 0.3125cm side lengths of small cubic box, respectively.

Figure 1 compares the scalar fluxes for three coarse cubes 1, 2, and 3. Figure 2 compares the scalar flux maps at the plane $y=2.5\text{cm}$. Figure 1 shows that the LDEM-SCB ($\lambda=1.0, 0.9, 0.8$) solution converges faster than DFEM for the coarse cube 1 and 2 scalar fluxes while DFEM solution converges faster than LDEM-SCB for the coarse cube 3 flux. It is noted that LDFEM-SCB ($\lambda=0.6$) gives larger value of scalar flux for the coarse cubes 1 and 2 while it gives smaller one for the coarse cube 3 in which the flux is small. Although the scalar flux for the coarse cube 4 is not given here, the negative fluxes for DFEM were found in the first and second mesh division cases while all the scalar fluxes for LDEM-SCB were positive for all the cases. Our experiences for several problems show that LDFEM-SCB gives robust solutions in terms of positivity than DFEM while it overestimates the scalar flux for the low flux regions near boundaries. At present, LDFEM-SCB uses only face average fluxes but it is possible to use a higher-order expansion of flux. In the future, we will consider this option in order to improve the accuracy.

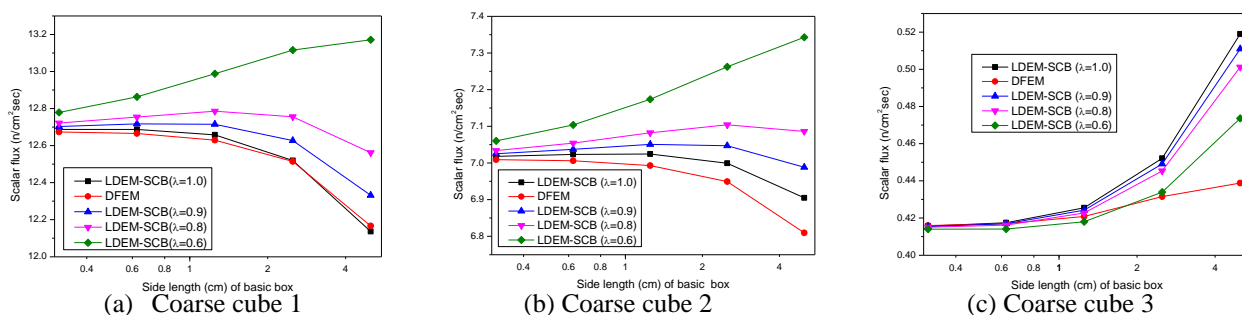


Fig. 1. Comparison of the region-wise scalar fluxes versus the mesh division

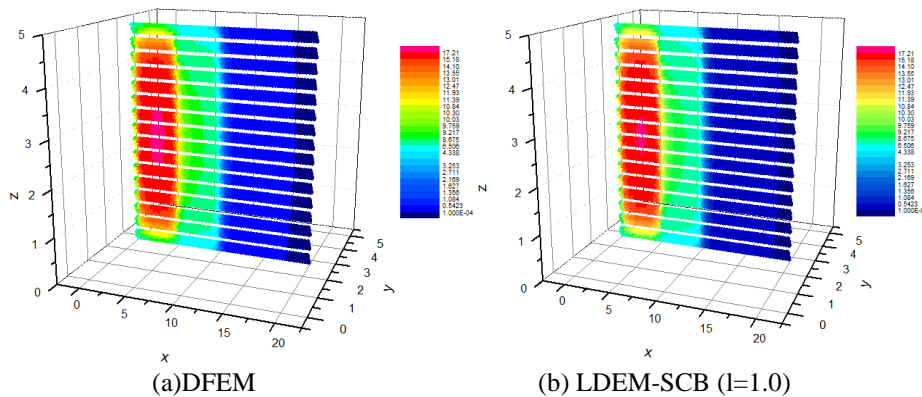


Fig. 2 Comparison of the plane scalar flux maps ($y=2.5\text{cm}$)

Acknowledgement

This work is supported by Agency for Defense Development (Contract No. UC080023GD).

REFERENCES

[1] J. E. Morel and E. W. Larsen, "A Multiple Balance Approach for Differencing the S_N Equations," *Nucl. Sci. Eng.*, Vol.105, p.1, 1990.

[2] M. L. Adams, "Subcell Balance Methods for Radiative Transfer on Arbitrary Grids," *Trans. Th. And Statistical Physics*, Vol. 26, p.385, 1997.
 [3] M. L. Adams, "Discontinuous Finite Element Transport Solutions in Thick Diffusive Problems," *Nucl. Sci. Eng.*, Vol.137, p.298, 2001.
 [4] T. A. Wareing, et al., "Discontinuous Finite Element S_N Methods on Three-Dimensional Unstructured Grids," *Nucl. Sci. Eng.*, Vol.138, p.256, 2001.